Chemical Physics Impact 5 (2022) 100100

Contents lists available at ScienceDirect

Chemical Physics Impact

journal homepage: www.sciencedirect.com/journal/chemical-physics-impact

Optimization of supercapacitive properties of polyindole by dispersion of MnO_2 nanoparticles

R.V. Barde [a,*], K.R. Nemade [b], S.A. Waghuley [c]

[a] Department of Physics, Government Vidarbha Institute of Science and Humanities, Amravati 444 604, India
[b] Department of Physics, Indira Mahavidyalaya, Kalamb, India
[c] Department of Physics, Sant Gadge Baba Amravati University, Amravati 444 602, India

ARTICLE INFO

Keywords:
Supercapacitive properties
Polyindole
MnO_2 nanoparticles
Optical band gap

ABSTRACT

This study demonstrates the dispersion of MnO_2 nanoparticles in Polyindole (PIn) to optimize the supercapacitive properties of MnO_2-PIn composites. As expected, the supercapacitive properties of MnO_2-PIn composites influenced by the addition of MnO_2 nanoparticles and it is optimized for 1 wt.% of MnO_2 concentration. The 1 Wt.% MnO_2 loaded PIn composite shows specific capacitance of the order 1558 Fg^{-1} at a scan rate of 50 mVs^{-1}. The main accomplishment of present work is that the 1 Wt.% MnO_2 loaded PIn composite shows long-term stability that is capacitance retention up to 6000 cycles. Galvanostatic charge/discharge curves of 1 Wt.% MnO_2 loaded PIn composite shows long nearly symmetric behavior which is suitable for range of practical applications.

Introduction

Globally, we are facing a huge problem about energy shortage due to rapid development of economy and increasing depletion of fossil fuels [1]. Hence, there is a crucial need for development new energy sources. Now a days, supercapacitors as high-performance energy storage devices offer a great promise in the field of energy storing technology because of its remarkable properties that is high charging and discharging rates, excellent power density, good stability and excellent long-term cyclability [2–4]. Nevertheless, to meet the requirement of budding applications like electric vehicles, energy density of supercapacitor still need some improvement. Increasing the window working potential, which primarily related with the employed electrolyte is a cogent way to increase energy density of supercapacitor as energy density of it is proportional to the square of operating potential window and specific capacitance. In supercapacitors, active materials play a vital role in an electrochemical performance [5]. Recently, more devotion has been given on the growth of electrode materials of supercapacitor and it is a crucial component which determines the performance of supercapacitor. The carbon materials, metal oxides and conducting polymers have been most commonly used for the growth of electrode as they exhibit such supercapacitor behavior [6–7].

Among these metal oxide MnO_2, is considered to be the most auspicious one because of its characteristics like higher specific capacitance, environmentally friendly, natural abundance and economical [8–9]. Despite of this, it has some drawbacks like poor ionic and electronic conductivity, less specific surface area and partial dissolution in the electrolyte during cycling which limiting the practical applications of MnO_2 in supercapacitors [10]. Hence for researcher it is a significant task to overcome these disadvantages of MnO_2. Dai et al reported nanobelt-structured MnO_2 films which were prepared by the electrochemical deposition method under various deposition time to explore the effects of electrodeposition time change on the microstructure and electrochemical properties of this material. Result show that the optimum sample deposited for 50 s has a specific capacitance of 291.9 F g^{-1} at the current density of 1 A g^{-1} [11]. In addition, Zhanga et al reported the structure and electrochemical performance of MnO_2 and MnO_2/reduced graphene oxide electrode materials which shows the capacitance of 467 F g^{-1} [12].

Conducting polymers are fascinating materials for fundamental and applied researches due to their 1D intrinsic properties and remarkable applications such as field effect transistor (FET), displays, rechargeable batteries, etc. [13]. Among various conducting polymers, comparatively polyindole has been less studied as it has low polymerization efficiency. Recently polyindol (PIn) has received enormous attention because of its good environmental stability and electrical conductivity [14]. As it is

* Corresponding author.
E-mail address: rajeshbarde1976@gmail.com (R.V. Barde).

https://doi.org/10.1016/j.chphi.2022.100100
Received 6 April 2022; Received in revised form 21 May 2022; Accepted 21 July 2022
Available online 23 July 2022

well known that Polyindole has benzine and pyrrrol ring, also these polymers have good thermal stability, low degradation rate and high storage capacity [15]. Due good electrocatalytic activity of Polyindole it has been reported in mediated based biofuel cell [14]. Polymer-metal oxide nanocomposite synthesis is incipient research as it has a remarkable technological applications like rechargeable batteries, fuel cells, and super capacitors [16]. Polyindole and its derivatives attract the researcher to take curiosity in the field of nanocomposites due to interesting properties. Nanoparticles of metal oxide such as copper and silver when doped in polyindole shows good antibacterial activity [17].

In the light of above discussion, we planned to investigate the supercapacitive properties of MnO_2-PIn composites. In this work, we studied the supercapacitive properties such, cyclic voltammetry (CV) curve, cycle stability performance and galvanostatic charge/discharge curves of composite materials. The main accomplishment of present work is that we achieved considerable values of specific capacitance, cycle stability and charging/discharging time.

Experimental

Materials

Indole, manganese dioxide, ferric chloride and ethanol (AR grade, 99% purity, SD Fine) were procured from local chemical supplier. Throughout the synthesis double distilled (DD) water was used to prepare the solution.

Synthesis of polyindole (PIn)

Oxidative polymerization method was preferred for the synthesis of polyindole (PIn) from indole in which ferric chloride used as oxidizing agent in aqueous medium. The aqueous solution (1M) was taken in a beaker and kept for continuously stirred on magnetic stirrer at normal temperature for 45 min. The ferric chloride solution (1M) was added dropwise manner to indole solution and stirred for 180 min. and then kept this mixture for overnight. The mixture was turn into dark brown which confirms formation of PIn. This mixture was filtered and to remove the impurities, precipitate was repeatedly washed with double distilled water. The obtained PIn was dried out at 60°C for 4 h and by using mortar and pestle the product was crushed.

Synthesis of MnO_2 nanoparticle

The nanoparticle of MnO_2 was prepared by sonication. A horn type 20 kHz Sonics sonifier with a tip diameter of 13 mm was used. Typically, 5 gm of MnO_2 was dissolved in 100 ml of double distilled water and kept for continuous stirring for 20 min. and then this mixture was ultrasonicated for 30 min. a brown color precipitate was formed. This precipitate was filtered, washed in double distilled water and then wash by ethanol and dried out in an air oven at 100° C for 4 h.

Synthesis of PIn/MnO_2 composites and characterizations

PIn doped with MnO_2 nanoparticles was synthesized by using an ethanolic solution of PIn and MnO_2 by varying concentration of MnO_2 with fixed PIn using Ex-situ technique in wt.% stichometry with the interval of 0.25 wt.% [18]. The composites preparation range was fixed from 0.25 to 1 wt.%. The as such prepared composites were nomenclature as 0.25 wt.% MnO_2 as (PM1), 0.5 wt.% MnO_2 as (PM2), 0.75 wt.% MnO_2 as (PM3) and 1 wt.% MnO_2 as (PM4). This prepared samples were used for further study of supercapacitor and ultraviolet–visible spectro-photometer.

By using Bruker D8 advance with Cu Kα radiation the phase purity and structure of as prepared samples were confirmed in which the pattern recorded with step height of 0.02° with scan rate 6.00 in the range 10°−80°. Morphologies of all samples were studied by using JEOL-6390LV scanning electron microscope. Ultraviolet-visible spectrophotometer was used to record the complex optical properties of all prepared samples, from which the values of optical band gap was calculated. The FTIR was taken in the KBr medium at room temperature in the region 4000−500 cm^{-1} at scan rate 16. Supercapacitor property measurements such as cyclic voltammetry (CV) curve, cycle stability performance and galvanostatic charge/discharge curves were carried out using three-electrode cell systems (CHI 660 D, CH Instruments). The composites systems under study were used as the working electrode, platinum wire as counter electrode and Ag/AgCl as the reference electrode.

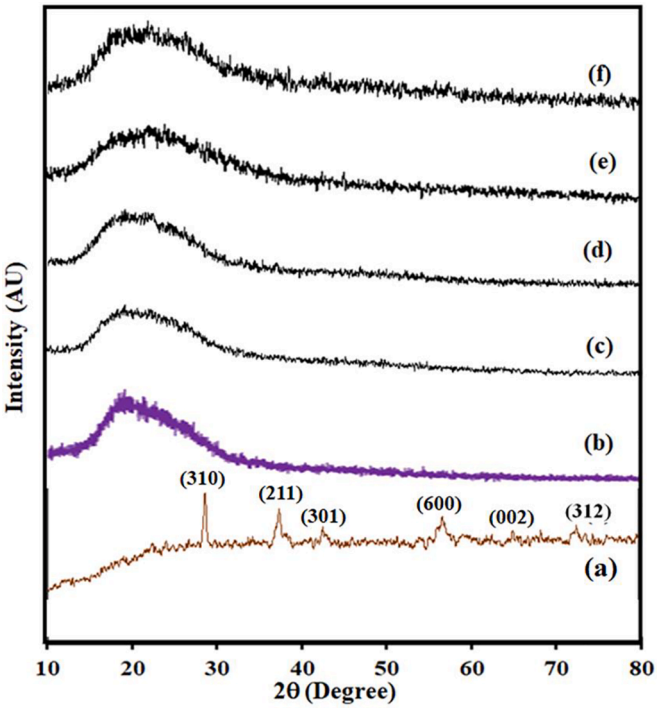

Fig. 1. XRD pattern of (a) MnO_2 nanoparticle material, (b) Pure PIn, (c) PM1, (d) PM2, (e) PM3 and (f) PM4 composites.

Results and discussion

XRD analysis

XRD patterns of MnO_2 nanoparticles, Pure PIn and PIn/MnO_2 composites were recorded at normal temperature in two theta range 10°–80°. Fig. 1 depicts the diffractogram of MnO_2 nanoparticles (Fig. 1 a), Pure PIn (Fig. 1 b) and PIn/MnO_2 composites (Fig. 1 c, d, e and f). All diffraction peaks of undoped MnO_2 nanoparticles corresponded well to tetragonal crystal symmetry of MnO_2 (ICDD: 44–0141). Diffraction peaks observed at 28.81°, 37.45°, 42.95°, 56.73°, 65.36° and 72.70° and these values corresponds to (310), (211), (301), (600), (002) and (312) planes [19–20]. The mean crystallite size of MnO_2 was found to be 23.45 nm calculated by using Debye-scherrer formula:

$$D = \frac{k\lambda}{\beta\cos\theta}$$

where k is Scherrer constant, λ is wavelength of X-ray, β is full width half maxima and θ is the Bragg's angle.

In Fig. 1(b), the broad peak appears in between 15° to 30° is the characteristic peak of the amorphous PIn, indicating the presence of PIn [21]. No evident peaks for MnO_2 were observed in XRD patterns of MnO_2/PIn composite. This could be a part of distortion in crystal structure of MnO_2 and also may be that MnO_2 particles were covered by

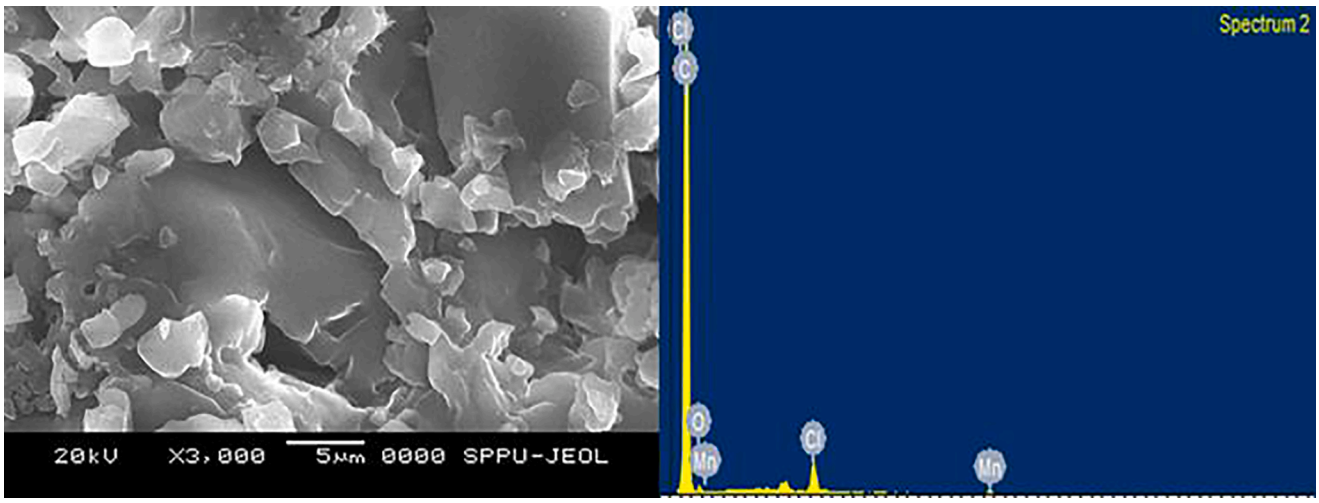

Fig. 2. SEM and EDAX image of PM4 composite.

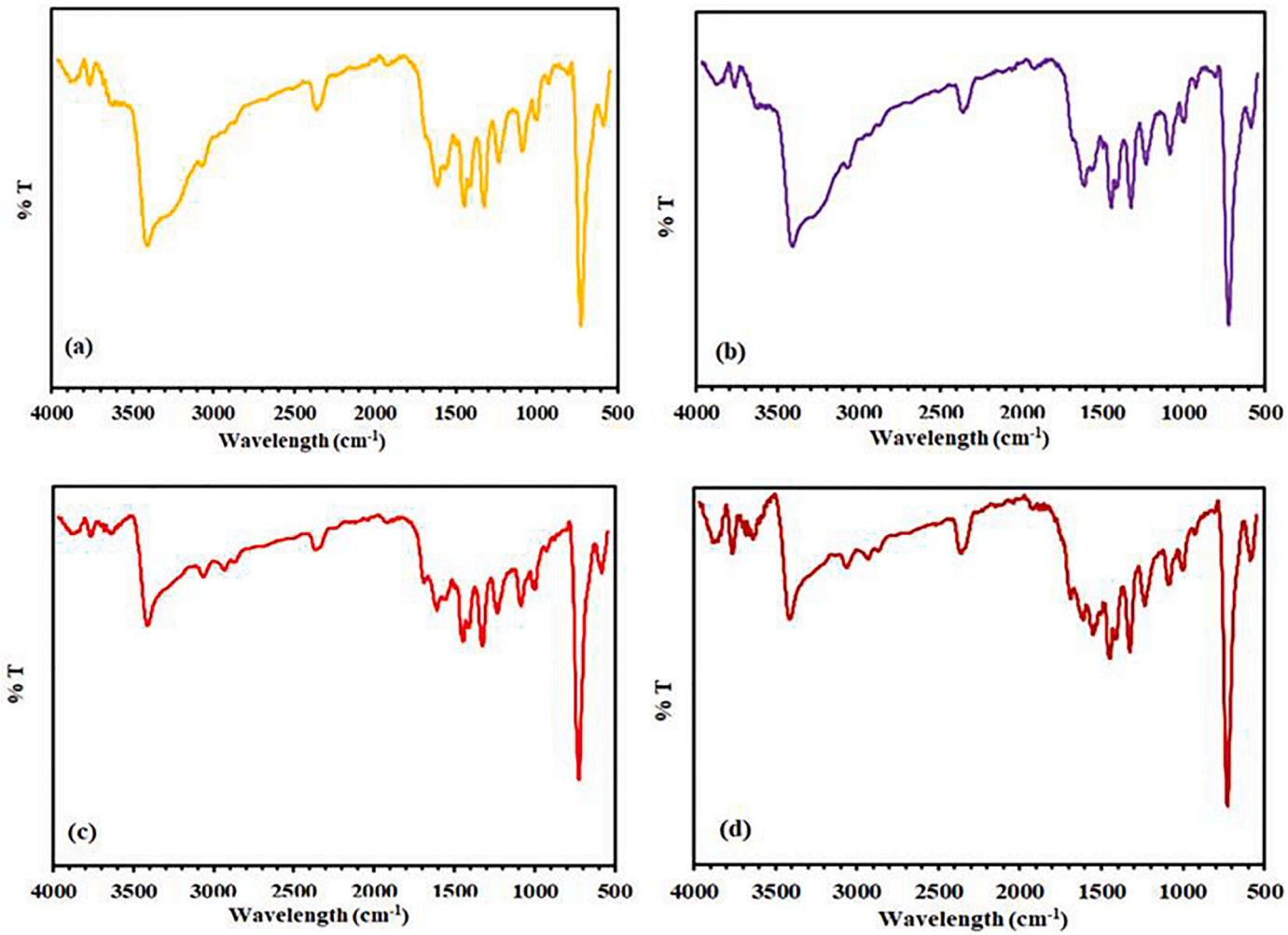

Fig. 3. FTIR spectra of (a) PM1, (b) PM2, (c) PM3 and (d) PM4 composites.

PIn.

SEM and EDAX study

The SEM proposed an external morphology of prepared samples. Fig. 2 shows the SEM and EDAX image of PM4 composite. SEM shows that composites have an irregular shape particle [22]. The EDAX spectrum of PM4 composite gives the confirmation about the presence of Manganese (Mn) and oxygen (O). Also, some impurities found during the preparation of composites which was removed by annealing process.

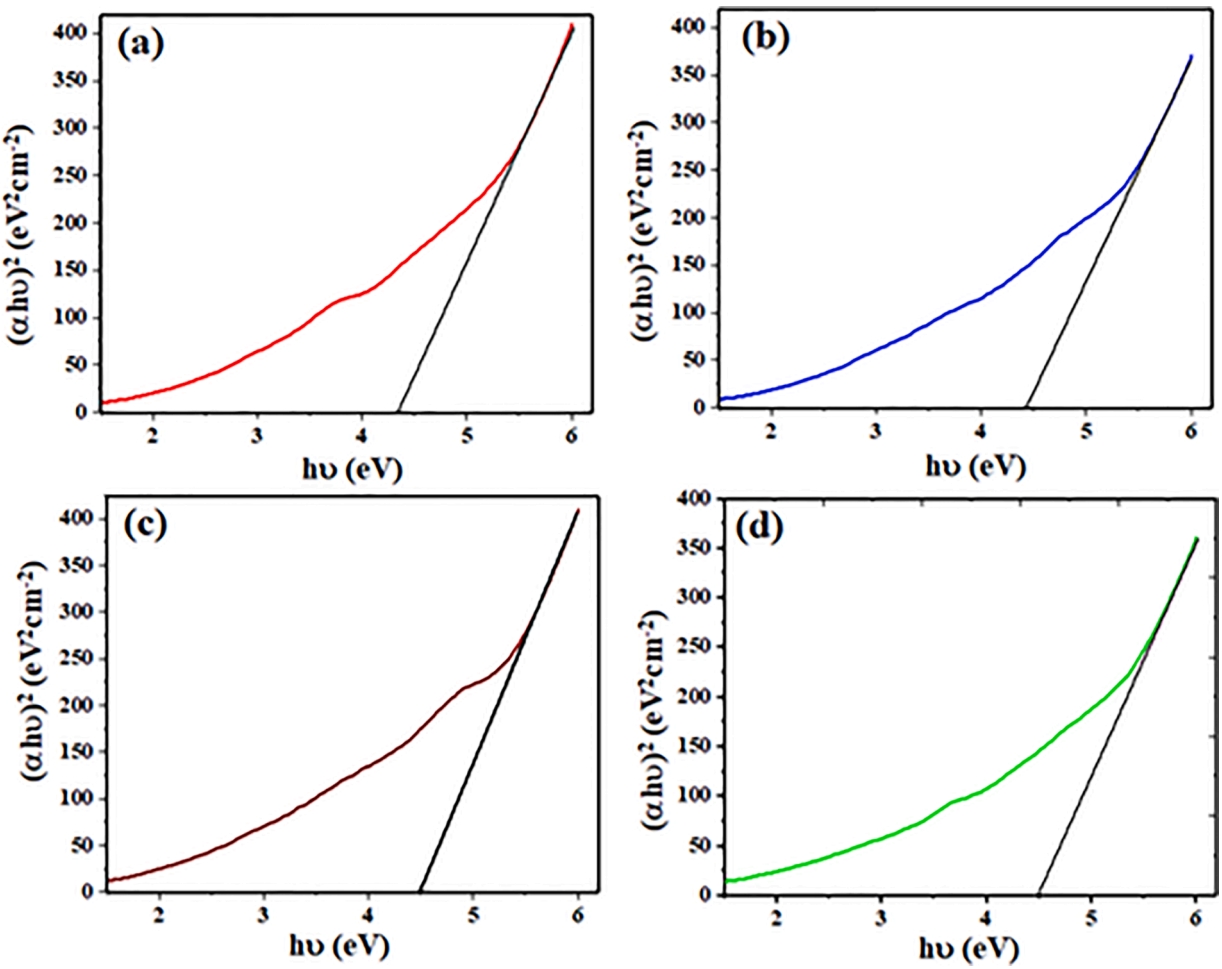

Fig. 4. Tauc plots of (a) PM_1, (b) PM_2, (c) PM_3 and (d) PM_4 composites.

The peak due to oxygen in EDAX confirms the oxygen storage capacity of prepared composites. As EDAX shows the existence of small amount of Mn and due to this reason MnO_2 was not detected by XRD.

FTIR study

Fig. 3 depict the FTIR spectrum of PIn/MnO_2 for all composites. A small peak at 530 cm^{-1} was assigned with Mn–O stretching [23]. Also, the peak at 600 cm^{-1} indicates the characteristic stretching collision of O–Mn–O, which confirmed the existence of the MnO_2 in the sample [24–25]. A strong peak observed at 742 and 1467 cm^{-1} are corresponding to the benzene ring, which indicates that the benzene ring did not involve in the polymerization [26–27]. The peak located at 1100 cm^{-1} is induced by different stretching frequencies of aromatic ring in the polymer chain, which corresponds to the stretching mode of C=N bond [28]. The peaks observed at 1336 and 1010 cm^{-1} shows the stretching mode of pyrrole ring and vibration mode of C–N bond [27]. The peak near 1236 cm^{-1} shows the surface OH groups of Mn–OH [24]. The peak 1559 cm^{-1} together with 3436 cm^{-1} can be ascribed to N–H bond stretching and deformation vibrations shows that nitrogen species are not the polymerization sites, hence the possibility of polymerization is through 2 and 3 position of indole monomer [29–30]. The peaks appear at 1630 cm^{-1} can be attributed C=O stretching vibrations [31].

Optical properties

The optical band gap gives idea about the energy to excite the electrons from outermost band to conduction band. The optical band gap of all PIn/MnO_2 composite was calculated from UV–visible spectroscopy ranging from 200 to 800 nm are shown in Fig. 4 (a, b, c and d). The Tauc plots were drawn to calculate band gap from following relation [32]:

$$\alpha h\vartheta = A\left(h\vartheta - E_g\right)^m$$

where A is an energy dependent constant, Eg is optical band gap of material, m is constant that depends on the semiconducting materials, which can be expected to have values of 1/2, 3/2, 2 and 3 depending on the nature of the electronic transition responsible for absorption; 1/2 for allowed direct transitions, 3/2 for direct forbidden transitions, 2 for allowed indirect transitions and 3 for indirect forbidden transitions [33]. Bandgap value of all samples was estimated by drawing $(\alpha h\upsilon)^2$ on y-axis and (hυ) on x-axis. hυ was calculated simply using the relation;

$$h\vartheta = \frac{1240}{\lambda(nm)}\ eV$$

The band gap was found out by extra plotting the straight line of graph. The point where extra plotting intersects the hυ axis (x-axis) gives band gap value. The highest band gap value was observed to be 4.50 eV for PM4 composite where as lowest band gap value was observed to be 4.33 eV for PM1 composite. The highest band gap was probably due to quantum confinement [34–35].

Supercapacitive study

Electrochemical energy storage capacitance of PM1, PM2, PM3 and PM4 composite as electrode of electrochemical capacitor was evaluated

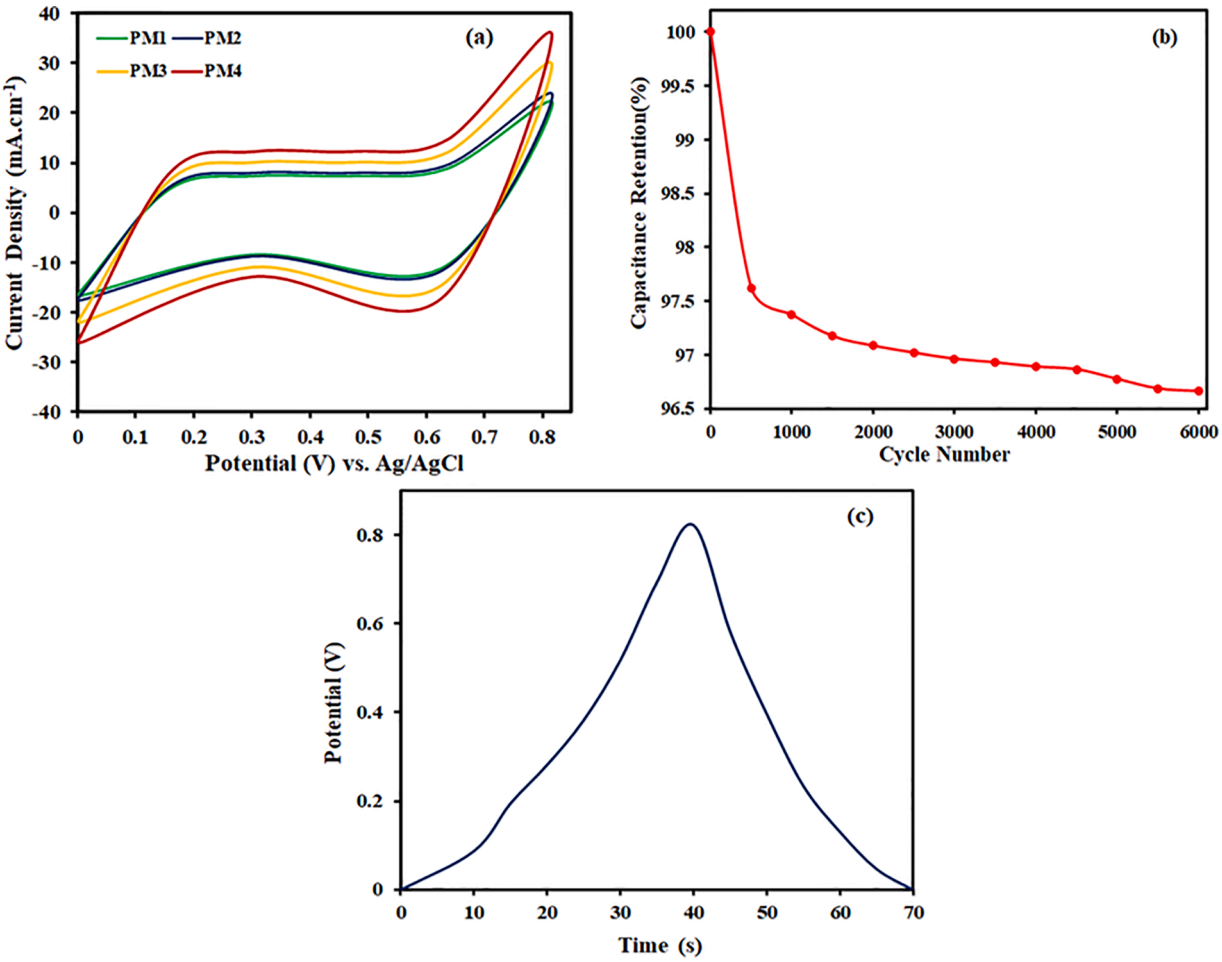

Fig. 5. (a) CV curves of PM1, PM2, PM3 and PM4 composites recorded at a scan rate of 50 mVs^{-1}, (b) Cycle performance of the PM4 composite 6000 cycles and (c) Galvanostatic charge/discharge curves of the PM4 composite recorded at a current density of 10 μAcm^{-2}.

from cyclic voltametric (CV) curves. Fig. 5 (a) illustrates the cyclic voltametric (CV) curves of PM1, PM2, PM3 and PM4 composite recorded at a scan rate of 50 mVs^{-1} in potential range of 0 to 0.8 V, which shows quasi-rectangular graphs indicating a pseudo-capacitive behavior and reversible doping/dedoping reactions [36]. The CV plots clearly shows the doping of MnO_2 nanoparticles in PIn influence supercapacitive properties composite. The superior supercapacitive properties of PIn/MnO_2 composite can be attributed to oxidation/reduction of surface hydroxyl groups [37]. The curve shape of PIn/MnO_2 composites are more rectangular, which shows a good capacitive behavior. Specific capacitance has been estimated using the relation [38]:

$$Cs = \frac{I}{m \times v}\left(Fg^{-1}\right)$$

where I is the average current during anodic and cathodic scan (A), m is the mass of the electrode (g) and v is the scan rate (V). In our case, the highest value of specific capacitance was found to be 1558 Fg^{-1} at a scan rate of 50 mVs^{-1} for PM4 composite which may be due to the porous structure of PIn/MnO_2 composites enhances specific capacitance.

Fig. 5(b) shows the PM4 composite exhibits considerable long-term stability that is capacitance retention up to 6000 cycles. The decent capacitance capability of PM4 composite is recognized to boosted electrical conductivity and vastly stable surface redox reaction and it is more suitable for electrode applications.

Fig. 5(c) shows the galvanostatic charge/discharge (GCD) curves of PM4 composite at current density 10 μAcm^{-2} within potential window 0 to 0.8 V. GCD curves of PM4 composite is nearly symmetric and considerably lengthy for practical application. The characteristic pseudocapacitive performance was indicated by nonlinear GCD curves, which may be due to the reversible redox reaction with insignificant loss of voltage and it suggest that electrolyte has excellent electrical conductivity between the current collector and active materials.

Conclusions

In summary, we have successfully demonstrated and concludes that concentration of MnO_2 nanoparticles in PIn composite have significant influence. The PM4 composite have specific capacitance of the order 1558 Fg^{-1} at a scan rate of 50 mVs^{-1} and also shows long-term stability that is capacitance retention up to 6000 cycles. The galvanostatic charge/discharge curves depicts that PM4 composite also have long and nearly symmetric behavior which is suitable for range of practical applications. The obtained results in this work attributed to the porous structure of PIn/MnO_2 composites.

Compliance with ethical standards

The submitted work is original and not submitted/published elsewhere in any form or in any other language.

Research data policy and data availability statements

The raw/processed data required to reproduce these findings cannot be shared at this time as the data also forms part of an ongoing study.

Author contribution

All authors contributed to the study conception and design. Material preparation, data collection and analysis were performed by Rajesh Barde. The first draft of the manuscript was written by Rajesh Barde, Sandeep Waghuley and Kailash Nemade and all authors commented on previous versions of the manuscript. All authors read and approved the final manuscript.

Author statement

We hereby declare that the submitted work is outcome of our original lab work and not published elsewhere also all the authors have given permissions for the submission. If present work found published elsewhere in any other language, I will be considered as a responsible person for the further actions.

The authors whose names are listed immediately below certify that they have NO affiliations with or involvement in any organization or entity with any financial interest (such as honoraria; educational grants; participation in speakers' bureaus; membership, employment, consultancies, stock ownership, or other equity interest; and expert testimony or patent-licensing arrangements), or non-financial interest (such as personal or professional relationships, affiliations, knowledge or beliefs) in the subject matter or materials discussed in this manuscript.

Declaration of Competing Interests

The authors have no relevant financial or non-financial interests to disclose.

Acknowledgements

The author acknowledges Director, Govt. Vidarbha institute of Science and Humanities, Amravati, Head, Department of Physics, Govt. Vidarbha institute of Science and Humanities, Amravati, and Head, Department of Physics, Sant Gadge Baba Amravati University, Amravati for providing necessary facilities for the work.

References

[1] Y. Zhang, Y. Mo, Preparation of MnO_2 electrodes coated by Sb-doped SnO_2 and their effect on electrochemical performance for supercapacitor, Electrochimica Acta 142 (2014) 76–83.
[2] C. Poochai, C. Sriprachuabwong, J. Sodtipinta, J. Lohitkarn, P. Pasakon, V. Primpray, N. Maeboonruan, T. Lomas, A. Wisitsoraat, A. Tuantranont, Alpha-MnO_2 nanofibers/nitrogen and sulfur-co-doped reduced graphene oxide for 4.5 V quasi-solid-state supercapacitors using ionic liquid-based polymer electrolyte, J. Coll. and Interf. Sci. 583 (2021) 734–745.
[3] A. Tyagi, K.M. Tripathi, R.K. Gupta, Recent progress in micro-scale energy storage devices and future aspects, J. Mate. Chem. A 3 (2015) 22507–22541.
[4] L. Chen, Z. Song, G. Liu, J. Qiu, C. Yu, J. Qin, L. Ma, F. Tian, W. Liu, Synthesis and electrochemical performance of polyaniline–MnO_2 nanowire composites for supercapacitors, J. Phys. and Chem. of Sol. 74 (2013) 360–365.
[5] M. Winter, R.J. Brodd, What Are Batteries, Fuel Cells, and Supercapacitors? Chem. Revi. 104 (2004) 4245–4269.
[6] C.B. Diaz-Arriaga, J.M. Baas-Lopez, D.E. Pacheco-Catalan, J. Uribe-Calderon, Uribe-Calderon, Symmetric electrochemical capacitor based on PPy obtained via MnO_2 reactive template synthesis, Synth. Met. 269 (2020), 116541.
[7] M. Ho, P. Khiew, D. Isa, T. Tan, W. Chiu, C.H. Chia, A review of metal oxide composite electrode materials for electrochemical capacitors, Nano 9 (2014), 1430002.
[8] X. Lu, T. Zhai, X. Zhang, Y. Shen, L. Yuan, B. Hu, L. Gong, J. Chen, Y. Gao, J. Zhou, Y. Tong, Z.L. Wang, WO3-x@Au@MnO_2 core-shell nanowires on carbon fabric for high-performance flexible supercapacitors, Adv. Mater. 24 (2012) 938–941.
[9] L. Bao, J. Zang, X. Li, Flexible Zn_2SnO_4/MnO_2 core/shell nanocable-carbon microfiber hybrid composites for high-performance supercapacitor electrodes, Nano Lett 11 (2011) 1215–1220.
[10] Z. Chen, V. Augustyn, J. Wen, Y. Zhang, M. Shen, B. Dunn, Y. Lu, High-performance supercapacitors based on tntertwined CNT/V_2O_5 nanowire nanocomposites, Adv. Mater. 23 (2011) 791–795.
[11] X. Dai, M. Zhang, J. Li, D. Yang, Effects of electrodeposition time on a manganese dioxide supercapacitor, RSC Adv. 10 (2020) 15860.
[12] M. Zhanga, D. Yanga, J. Lib, Effective improvement of electrochemical performance of electrodeposited MnO_2 and MnO_2/reduced graphene oxide supercapacitor materials by alcohol pretreatment, J. Ener. Stora. 30 (2020), 101511.
[13] S.P. Koiry, V. Saxena, D. Sutar, S. Bhattacharya, D.K. Aswal, S.K. Gupta, J. V. Yakhmi, Interfacial synthesis of long polyindole fibers, J. Appl. Poly. Sci. 103 (2007) 595–599.
[14] R. Perveen, S.Haque Inamuddin, A. Nasar, A.M. Asiri, G.M. Ashraf, Electrocatalytic performance of chemically synthesized PIn-Au- SGO composite toward mediated biofuel cell anode, Sci. Rep. 7 (2017) 13353.
[15] S.Mehtab Rita, M.G.H. Zaidi, K. Singha, B. Arya, T.I. Siddiqui, Polyindole based nanocomposites and their applications: A review, Mater. Sci. Res. India 16 (2019) 97–102.
[16] G. Rajasudha, A.P. Nancy, T. Paramasivam, N. Boukos, N. Vengidusamy, S. Arumaiathan, Synthesis and Characterization of Polyindole-NiO-Based Composite Polymer Electrolyte with $LiClO_4$, Int. J. Polym. Mater. 60 (2011) 877–892.
[17] V. Kumar, C. Jolivalt, J. Pulpytel, R. Jafari, F. Arefi-Khonsari, Development of Silver Nanoparticle Loaded Antibacterial Polymer Mesh Using Plasma Polymerization Process, J. Biomed. Mater. Res., Part A 101 (2013) 1121–1132.
[18] R.V. Barde, Preparation, characterization and CO_2 gas sensitivity of Polyaniline doped with Sodium Superoxide (NaO_2), Mate. Res. Bul. 73 (2016) 70–76.
[19] L. Feng, Z. Xuan, H. Zhao, Y. Bai, J. Guo, C. Su, X. Chen, MnO_2 prepared by hydrothermal method and electrochemical performance as anode for lithium-ion battery, Nano. Res. Lett. 9 (2014) 290–298.
[20] S. Sivakumar, L.N. Prabu, Synthesis and Characterization of a-MnO_2 nanoparticles for Supercapacitor application, Mate. Sci., Eng. Mate. Today: Proc. 47 (2021) 52–55.
[21] L. Yuan, C. Wan, L. Zhao, Facial *In-situ* Synthesis of MnO_2/PPy composite for supercapacitor, Int. J. Electrochem. Sci. 10 (2015) 9456–9465.
[22] K.S. Shaker, A.H. Abd Alsalm, Synthesis and characterization nano structure of MnO_2 via chemical method, Eng. and Techn. Jou. 36 (9) (2018) 946–950.
[23] Y. Kumar, S. Chopra, A. Gupta, Y. Kumar, S.J. Uke, S.P. Mardikar, Low temperature synthesis of MnO_2 nanostructures for supercapacitor application, Mat. Sci. for Ener. Tech. 3 (2020) 566–574.
[24] D. Jaganyi, M. Altaf, I. Wekesa, Synthesis and characterization of whisker-shaped MnO_2 nanostructure at room temperature, Appl Nano sci 3 (2013) 329–333.
[25] M. Pang, G. Long, S. Jiang, Y. Ji, W. Han, B. Wang, X. Liu, Y. Xi, Rapid synthesis of graphene/amorphous a-MnO_2 composite with enhanced electrochemical performance for electrochemical capacitor, Mater. Sci. Eng., B 194 (2015) 41–47.
[26] N.Shakeel Inamuddin, M.I. Ahamed, S. Kanchi, H.A. Kashmery, Green synthesis of ZnO nanoparticles decorated on polyindole functionalized-MCNTs and used as anode material for enzymatic biofuel cell applications, Scient. Rep. 10 (2020) 5052.
[27] M. Elango, M. Deepa, R. Subramanian, A.M. Musthafa, Synthesis, characterization, and antibacterial activity of Polyindole/Ag–Cuo nanocomposites by reflux condensation method, Poly. Plast. Tech. and Eng. 57 (2018) 1440–1451.
[28] K. Giribabu, R. Manigandan, R. Suresh, L. Vijayalakshmi, A. Stephen, V. Narayanan, Polyindole nanowires: Synthesis, characterization and electrochemical sensing property, Chem Sci Trans. 2 (2013) 13–16.
[29] H. Talbi, D. Billaud, G. Monard, M. Loos, Theoretical investigation of the monomer reactivity in polyindole derivatives, Synth. Met. 101 (1999) 115.
[30] J. Xu, G. Nie, S. Zhang, X. Han, J. Hou, S. Pu, Electrosyntheses of freestanding polyindole films in boron trifluoride diethyl etherate, J. Poly. Sci., Part A: Poly. Chem. 43 (2005) 1444–1453.
[31] T.L. Montanheiro, F.H. Cristovan, J.P.B. Machado, D.B. Tada, N. Duran, A. P. Lemes, Effect of MWCNT functionalization on thermal and electrical properties of PHBV/MWCNT nanocomposites, J. Mater. Res. 30 (2015) 55–65.
[32] Y. Hu, B. Hu, B. Wu, Z. Wei, J. Li, Hydrothermal preparation of ZnS:Mn quantum dots and the effects of reaction temperature on its structural and optical properties, J. Mater. Sci.: Mater. in Elect. 29 (2018) 16715–16720.
[33] R.V. Barde, Influence of CeO_2 content on complex optical parameters of phosphovanadate glass system, Spect. Acta Part A: Mol. and Bio. Spect. 153 (2016) 160–164.
[34] M.U. Khalid, M.F. Warsi, I. Shakir, M.F. Aly Aboud, M. Shahid, S.S. Shar, S. Zulfiqar, Zulfiqar, Al^{3+}/Ag^{1+} induced phase transformation of MnO2 nanoparticles from α to β and their enhanced electrical and photocatalytic properties, Ceram. Int. 7 (2020) 9913–9923.
[35] N. Rajamanickam, P. Ganesan, S. Rajashabala, K. Ramachandran, Structural and optical properties of α− MnO_2 nanowires and β− MnO_2 nanorods, AIP Conf. Proc. 1591 (1) (2014) 267–269.
[36] J.G. Wang, Y. Yang, Z.H. Huang, F. Kang, MnO_2/polypyrrole nanotubular composites: Reactive template synthesis, characterization and application as superior electrode materials for high-performance supercapacitors, Electrochim. Acta 130 (2014) 642–649.
[37] D. Choi, G.E. Blomgren, P.N. Kumta, Fast and reversible surface redox reaction in nanocrystalline vanadium nitride supercapacitors, Adv. Mater. 18 (2006) 1178–1182.
[38] B. Sethuraman, K.K. Purushothaman, G. Muralidharan, Synthesis of mesh-like Fe_2O_3/C nanocomposite via greener route for high performance supercapacitors, RSC Adv. 4 (2014) 4631–4636.